Chapter 4. Characterization of FA Reinforced PU Foam Core Sandwich Composites under Bending

This chapter presents the enhancement of the mechanical performance of the PU foam core sandwich composites by employing fly ash, an industrial waste, as a potential particulate reinforcement. The effect of FA inclusion on the morphology change in cellular structure of PUF core is studied elaborately. The morphological change in cellular structure of foam core with addition FA and its impact on mechanical performance is investigated by conducting shear test on foam core. The reinforced foam core sandwich composite performance under bending of sandwich composite is also taken into consideration. The effect of GFRP/CFRP face sheet on bending performance of sandwich composites is also included here. At last, which the help of scanning electron microscopy, morphological investigation is done to substantiate the changes in mechanical properties with FA addition to PUF core.

4.1. Physical Characterization

4.1.1. Density of Face Sheet and PUF Core

Density of a composite depends on the relative proportion of matrix and reinforcing materials and this is one of the most important factors determining the properties of the composites. The density of the GFRP and CFRP laminated face sheet have been determined as per ASTM standard D792-13 [196]. Figure 4.1 shows the density setup for the determination of laminated face sheet. The typical measurement of the specimen mass and the calculated density based on the principles of Archimedes is noted in Table 4.1. The respective density of the GFRP and CFRP specimens are averaged and found to be 1486.23 kg/m^3 and 1344.525 kg/m^3

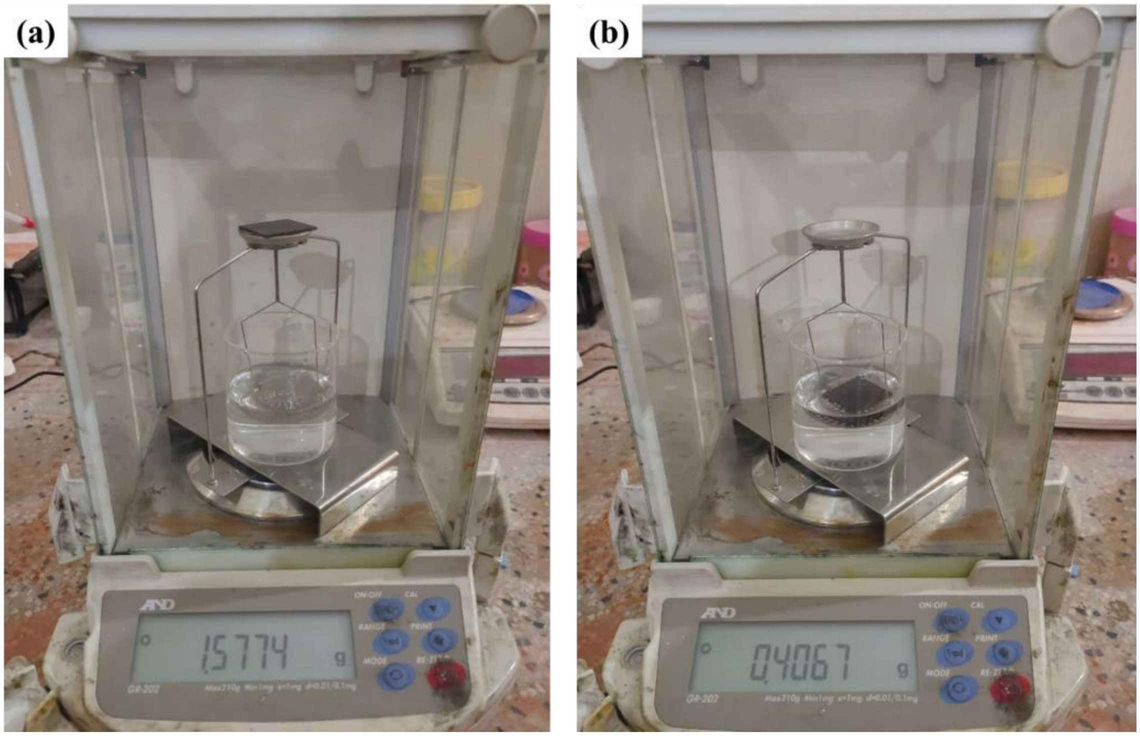

Figure 4.1 (a) mass of CFRP specimen in air (b) mass of CFRP specimen immersed in water

Table 4.1 Density calculation of GFRP and CFRP laminate face sheet

GFRP laminate face sheet				
S. No.	mass in air (Gram)	mass immersed in water (Gram)	Specific gravity	Density (kg/m^3)
1.	1.5556	0.5090	1.4863	1482.62
2.	1.5690	0.5185	1.4935	1489.84
CFRP laminate face sheet				
S. No.	mass in air (Gram)	mass immersed in water (Gram)	Specific gravity	Density (kg/m^3)
1.	1.5774	0.4067	1.3473	1343.93
2.	1.5940	0.4120	1.3485	1345.12

The core density of the PUF and reinforced FA-PUF sandwich composite was calculated according to ASTM D1622/D1622M [197]. Density has a substantial impact on the material's mechanical performance apropos the PUF prepared as a combination of two-component polyol and MDI in the prescribed ratio. The fly ash is introduced into the PUF matrix as particulate reinforcement. The amount of fly ash added to matrix material is 5%, 10%, 15% and 20% by weight of matrix material (Polyol + MDI). This inclusion leads to the density variation in PUF. The calculated density for different FA-PUF combinations is noted in Table 4.2.

Table 4.2 The calculated density for varying wt. % of FA to PUF.

Foam type	Neat PUF	5% FA-PUF	10% FA-PUF	15% FA-PUF	20% FA-PUF
Foam density (kg/m^3)	112.04	117.32	122.83	128.20	133.98

4.1.2. Particle Size Distribution of Surface Treated Fly Ash

Figure 4.2 shows the scanning electron microscopy of the fly ash particle before and after surface treatment with GPTS. From the SEM images, size of particles was calculated. Three samples were taken to measure the particle size distribution in fly ash. Since fly ash has been sieved after surface treatment, therefore, no particle with more than 53 μm size was seen in the treated fly ash. The FA constituent has mostly 42.02% particles below 2.5 μm size and 39.69% particles between 2.5 to7.5 μm size. These two comprise more than 80% of fly ash. Apart from this, 9.73% and 4.28% of particles were in the range of 7.5 to 12.5 μm and 12.5 to 17.5 μm, respectively. Only 5% of particles in fly ash were seen to be bigger than 17.5 μm. Figure 4.3 shows the particle size distribution of surface-treated fly ash.

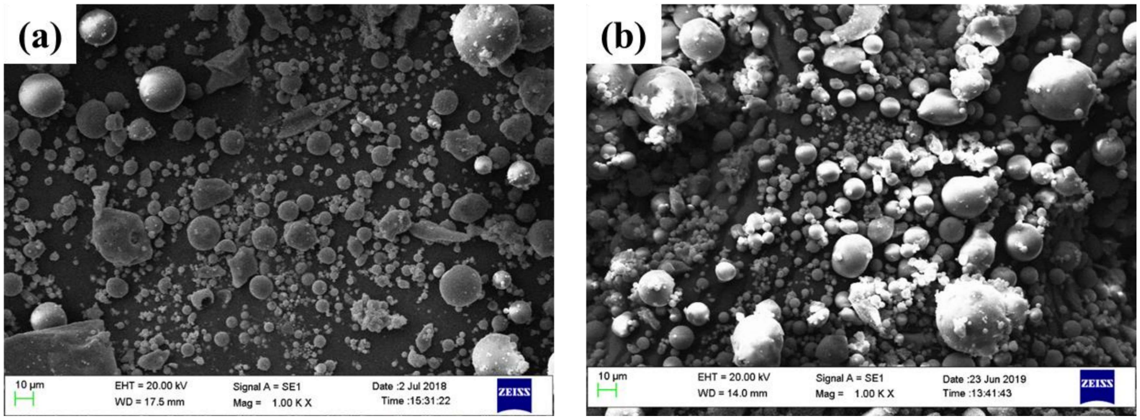

Figure 4.2 SEM image of Fly ash (a) before and (b) after surface treatment with GPTS

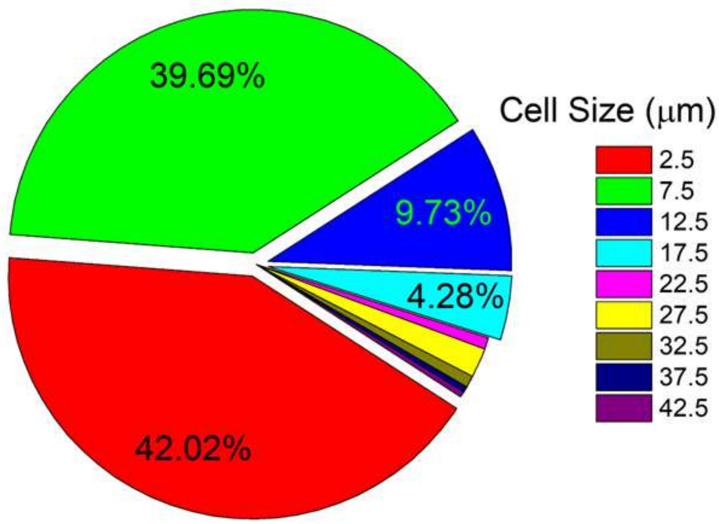

Figure 4.3 particle size distribution of treated fly ash.

4.2. Mechanical Characterization

In the present investigation, fly ash particulate has been used as reinforcement for improving the mechanical property of polyurethane (PU) foam core and PU based sandwich FRP composites. In the first part, test samples of PU foam core with different weight percentages (5% to 20% variation) of fly ash inclusion were prepared. The interfacial adhesion characteristics have been improved while initially treating the surface with 3-

Glycidyloxypropyl-trimethoxysilane (GPTS). In the second part, these reinforced PU were used as a foam core with glass fiber reinforced polymer (GFRP), and carbon fiber reinforced polymer (CFRP) face sheets to construct sandwich composite ASTM C 393/C393M-16 three-point bend specimens.

4.2.1. Tensile Test of GFRP and CFRP

Tensile specimens of the GFRP and CFRP laminate were cut from the parent laminate of the required size, as mentioned above. The specimen was clamped in the tensile grips and put under tensile loading condition with a constant strain rate of 0.5mm/min. Since GFRP and CFRP are brittle materials, these two did not undergo any plastic deformation as it is clear from the stress-strain curve Figure 4. 4. Five specimens of each GFRP and CFRP, undergo the tensile test at the same strain rate. The failure of GFRP and CFRP, according to the ASTM D3039/D3039M-17[198] can be categorized as mentioned in the ASTM standard. The failure in five specimens of GFRP is Lateral-at-Grip/Tab-Top (LAT) - 2 specimens, Lateral-at Grip/Tab- Bottom (LAB) – 2 specimens and Lateral-Gage- Middle(LGM) -1 Specimen[198]. Likewise, failure in CFRP is Lateral-at Grip/ Tab Various (LAV) - 4 specimen and Explosive-Gage-Middle (XGM) - 1 specimen. These failure modes are visible in the specimens in Figure 4.5 (a) and (b).

The average strength of GFRP is evaluated to be 142.38 MPa and its elastic modulus is 7.209 GPa. The average strength of CFRP is 423.7 MPa and the elastic modulus is 27.440 GPa. The strength of CFRP specimens is almost three times more than the GFRP specimen, while the elastic modulus of CFRP is more than three times to the GFRP. Strain at failure is higher for GFRP than the CFRP as shown in Figure 4.4.

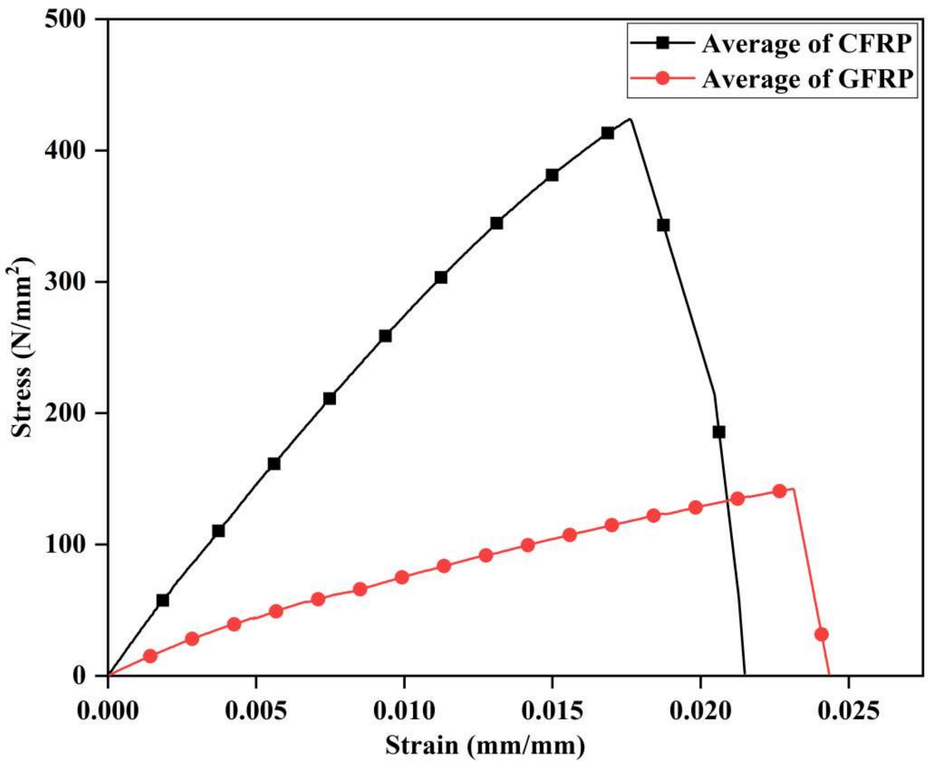

Figure 4.4 Comparison of average stress-strain of GFRP and CFRP under tensile loading.

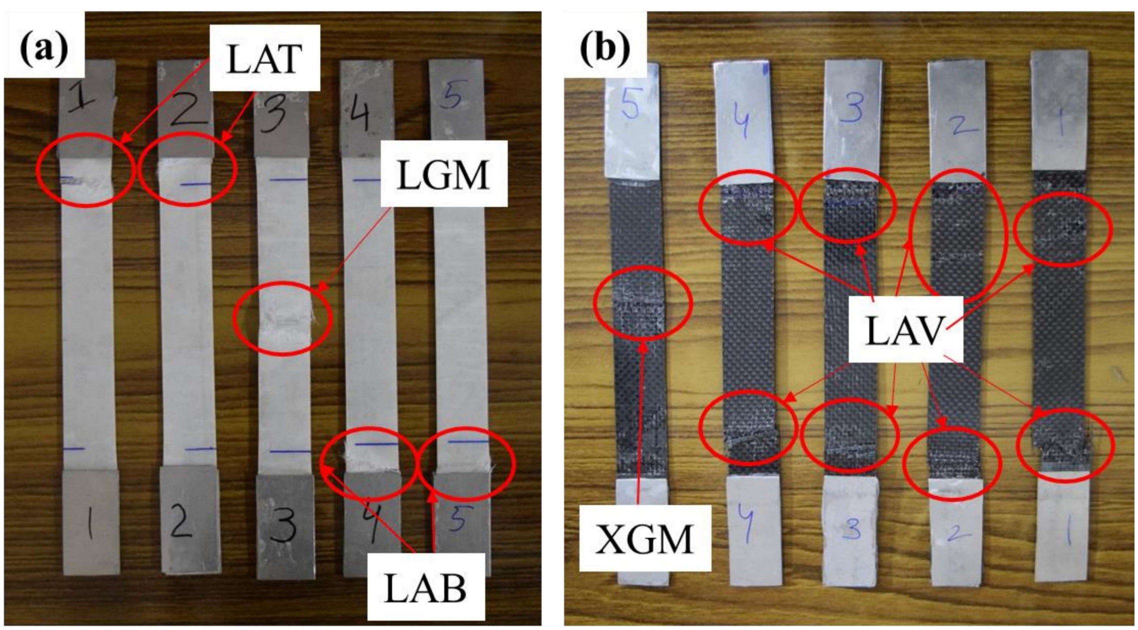

Figure 4.5 Failure mode of (a) GFRP (b) CFRP specimens under tensile loading.

4.2.2. Shear Test of Polyurethane Foam Core

Shear test is conducted on the PU foam core of the sandwich composites, and PU foam core is reinforced with the FA particulate. Since, silanes are known to increase the wettability of ceramic glass surfaces, it thus reduces the contact angles of the structure[47]. Earlier researches have shown that, a silane monolayer is said to be 10–50 nm thick. However excess of successive or thick layers of silane causes cohesive destruction between the layers of silane, thereby reducing the mechanical strength of the structure[53, 54]. But an ultra- thin layer of silane can cause weak mechanical bonding and can be ineffective to improve the mechanical interfacial properties. Therefore, to achieve enhanced mechanical properties of the fibre-reinforced composites, an optimal silane coating thickness is preferred. Therefore, it became necessary to conduct mechanical testing to verify whether, the FA reinforcement is actually enhancing or degrading the mechanical performance.

4.2.2.1. Comparison of surface treated and untreated FA-PUF specimens

Experimentation was conducted to assess the influence of surface treatment on the mechanical behaviour of fly ash included polyurethane (FA-PUF) shear specimens. Though the cost of PUF composite specimens increases with the surface treatment of FA with GPTS, the mechanical advantage obtained is worth noting. The surface treatment enhances the interfacial bonding and affinity of the particle for the matrix with uniform distribution and thereby improves the strength of the composite specimen. The use of silane (GPTS) improves the distribution of reinforcement particles in the polymer and the bonding between the reinforcement and polymer. This improvement in the distribution and bonding of FA to matrix leads to the superior mechanical performance of PUF structure. The mechanism of such improvement is also reported in previous literature, where the surface treatment of reinforcement using silane gave better results than the untreated specimens [59-61, 168, 203, 204]. PUF specimens were prepared with untreated fly ash as reinforcement. Then the untreated fly ash polyurethane foam (UTFA- PUF) is investigated under shear loading. From the stress-strain diagram of Figure 4.6, the degradation in strength and modulus in comparison to the treated fly ash polyurethane (TFA-PUF) is quite evident. The strength and modulus of UTFA-PUF are reduced by 15.58% and 5.49%, respectively. This reduction in strength and modulus ascribed to the weak interfacial bonding and agglomeration of fly ash. This low interfacial bonding hinders the stress transfer from the matrix to reinforcement particles. The SEM images of Figure 4.7 for the untreated UTFA-PUF also corroborate the findings. From the scanning electron microscopy images, agglomeration of FA particles at the strut and its non-uniform distribution in the cell wall is observed. This non-uniform distribution and agglomeration severely deteriorate the mechanical performance of the PUF sandwich composites. The stiffness of neat PUF is found to be less than the surface-treated FA-PUF core (TFA-PUF).

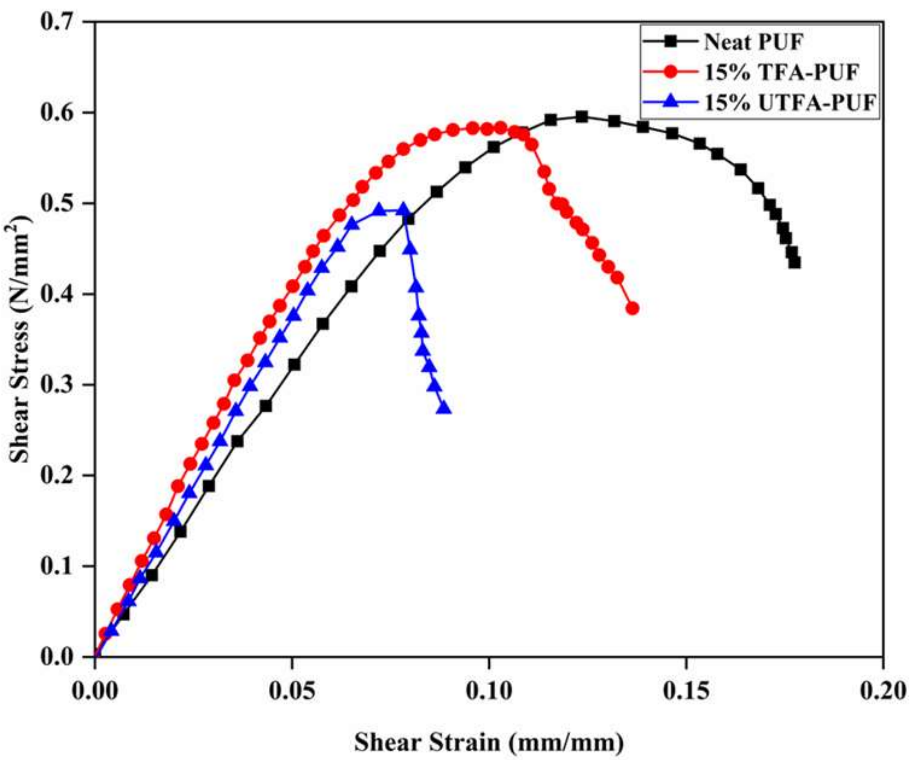

Figure 4.6 Shear stress-strain curve of neat PUF and 15 % of treated and untreated FA-PUF

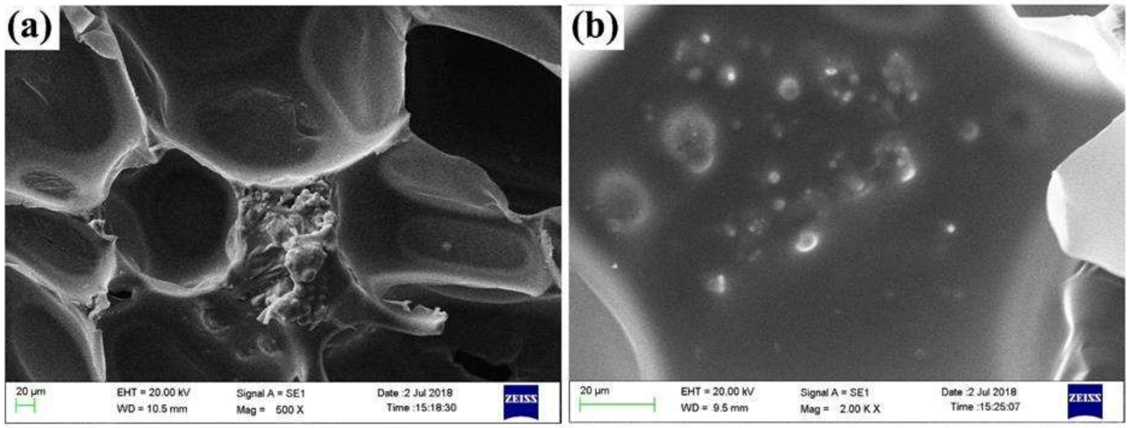

Figure 4.7 SEM of 15% UTFA-PUF specimen (a) SEM image showing agglomeration of FA particles at strut and (b) SEM image showing non-uniform distribution of FA particle in cell wall.

4.2.2.2. Shear test of neat and FA-PUF core

According to the ASTM standard C273/C273M – 16 [200], shear testings were conducted to obtain stress-strain behaviour of FA-PUF core with 5% to 20% of fly ash particulate inclusion. Shear tests on three samples of each category were carried out to get the average of each category of PUF core. From the stress-strain diagram of Figure 4.8 (a), it is observed that at 5% of fly ash inclusion, there is a decrease in strength in the PUF core though shear modulus is increased. Typically, at a saturated threshold FA inclusion of 10% and above up to 20%, both strength and shear modulus were found to increase. Table 4.3 lists the shear properties for all four categories of FA-PUF specimens. Failure modes were defined as described in ASTM standard C273/273M -16. Figure 4.8 (b) shows the failure mode in 10% FA-PUF core which is Shear at Gauge in Middle (SGM). Mode of failure is same for for all cases. The shear stress variation is linear till the maximum limit for all types of specimens. The 20% FA inclusion provides higher stiffness and strength against shear loading.

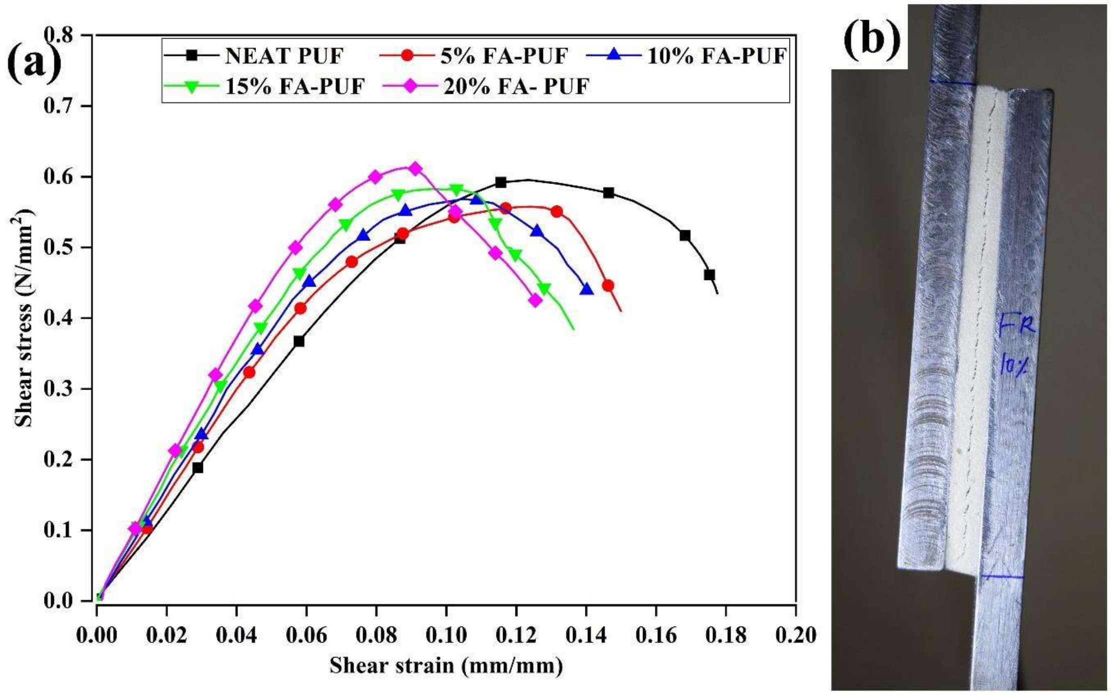

Figure 4.8 (a) Shear stress-strain curve of different weight % of fly ash loaded PUF (b) SGM failure in 10 % FA-PUF core.

Table 4.3 Different weight % of FA reinforced PUF and its shear strength and failure mode.

Type of Foam	Shear Strength (MPa)	Shear Modulus (MPa)	Failure code
Neat PUF	0.59	6.53	SGM (3 Sample)
5% FA-PUF	0.55	7.47	SGM (3 Sample)
10% FA-PUF	0.56	7.66	SGM (3 Sample)
15% FA-PUF	0.58	8.08	SGM (3 Sample)
20% FA-PUF	0.61	9.12	SGM (3 Sample)

4.2.3. Bending Test on Sandwich Composite

The three-point bend testing was performed according to ASTM standard C393/C393M-16 [201] for both GFRP and CFRP sandwich specimens having FA-PUF core as described earlier. The Load-deflection behaviour of the neat PUF without fly ash addition and fly ash (5 -20% variation) reinforced PUF with face sheets of GFRP and CFRP are shown in Fig.

4.9 and 4.11. The behaviour for all specimens is found to be linear, ascending up to the maximum load. The drop in load characteristics is due to the initiation of damage in FRP sandwich composites. However, the damage mechanisms are different for GFRP face sheet FA-PUF core sandwich and CFRP face sheet FA-PUF core sandwich composite specimens.

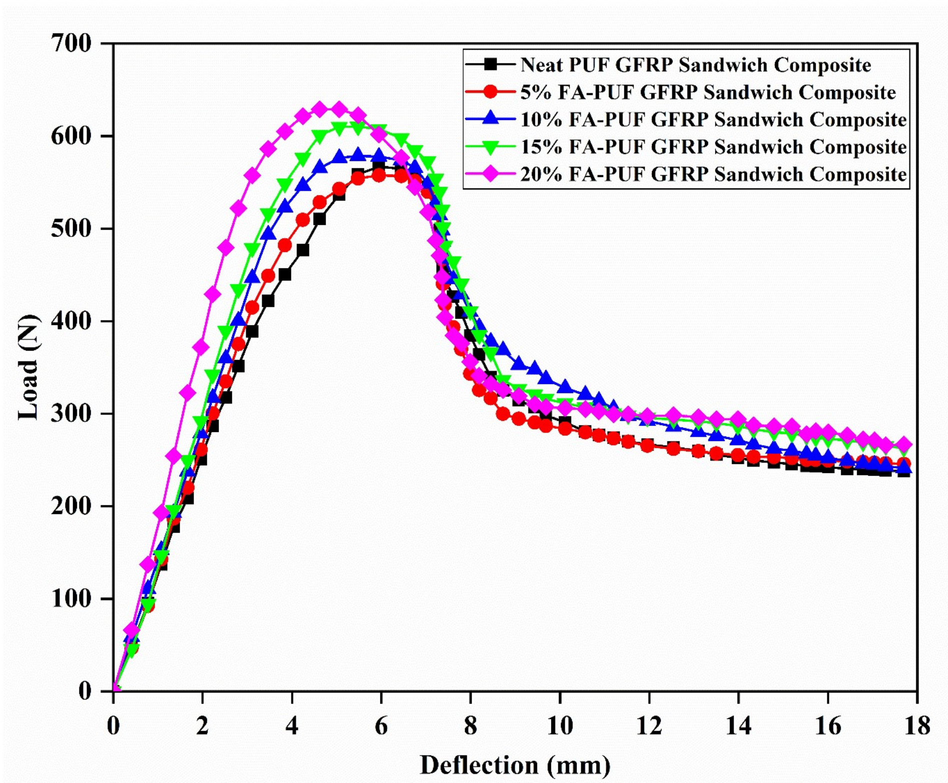

Figure 4.9 Load- Deflection curve of GFRP sandwich composite under bending.

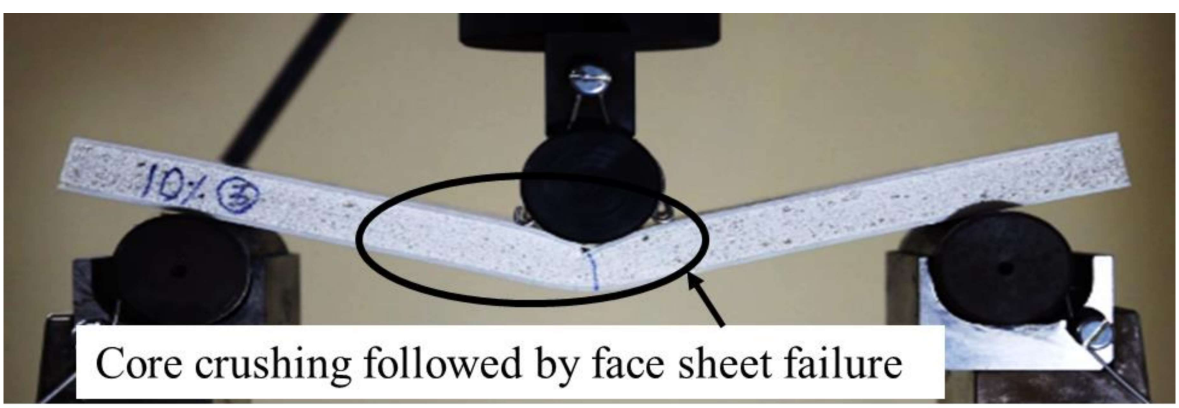

Figure 4.10 Failure of 10% FA-PUF GFRP composite under bending.

As shown in Figure 4.9, the slope of the load-deflection curve is increasing with the increase in weight percentage of the fly ash. The peak load is increased, corresponding to FA inclusion varying from 5% to 20% in FA-PUF sandwich composite. This suggests the improvement of stiffness of the GFRP sandwich composite with the addition of the fly ash. During bending of face sheet, foam compaction is also noticed in the sandwich specimens. This can be reasoned to the low stiffness of GFRP face sheets. The damage mechanism observed during the bending of the GFRP sandwich specimen is the top face sheet fails first at the roller due to indentation where the maximum load is transferred on the sandwich specimen. This leads to the drop in maximum load. This indentation failure of the top GFRP face sheet leads to the crushing of the core in between with the continuation of bending load further. In the meantime, the bottom face sheet is found to be intact with PUF core and thus sharing the major load proportion. The failure discussed can be seen in figure 4.10. Due to the failure of GFRP top face sheet and core crushing, load-carrying capacity reduced drastically with deflection, as evidenced in figure 4.9.

Though a similar load vs. deflection curve is obtained in the three-point bend test of CFRP sandwich composite (Figure 4.11), but the initiation of failure and damage mechanism after maximum load attained are fundamentally different. Here, the core failure precedes interfacial debonding of the face sheet with core. Till maximum load, there has been a linear variation of load with displacement. The flexural stiffness and strength are increased with the percentage addition of fly ash, as indicated by the increment in the slope of the load-deflection curve. A limit on the percentage of fly ash inclusion can be ascertained, because with the increment of fly ash weight percentage, the core becomes more rigid, leading to the sudden drop of load after maximum force and flexibility as delineated in the Figure 4.11 for the 20% FA-PUF specimen. Table 4.4 provides the peak bending load and corresponding deflection of GFRP and CFRP sandwich composites proportionate with the variation of weight % fly ash inclusion to the PUF core. During the flexure loading, shear load is transferred to the PUF core. Since, in contrast to GFRP face sheet, the CFRP is almost three times stronger, transverse shear failure of PUF core is observed first after peak load. Here, neither the top nor the bottom face sheet is cracked, while the shear damage was progressing through core. The shear stress that causes this mode of failure is perpendicular to the neutral plane bending. This pattern of failure due to transverse shear of cellular core sandwich composites under bending was also reported by Gibson and Ashby [88]. Since shear load is transferred to the PUF core; hence effectively core is also contributing to the stiffness of the beam. A similar failure mechanism was also observed for the 3-point bend testing of Aluminum foam core sandwich composite by Banghai et al. [205]. This was also verified by drawing equally spaced perpendicular lines to the neutral plane on the sandwich beam. Subsequent to bending, the drawn lines on the sandwich beam were found to be no longer perpendicular to the neutral plane but inclined to the neutral plane. The shear cracks appeared along these transverse shear lines corroborating that the shear failure in the core is because of transverse shear stresses as similarly observed in the present work.The shear failure in the foam core can be seen in figure 4.12 (a). The shear failure in the FA-PUF core further leads to debonding between the core and CFRP face sheet. This debonding induces a sudden decrease in peak load, as reflected in the plot Figure 4.11. This transverse shear failure of the core progresses further with persistent bending load resulting in the debonding of face sheet and core can be seen in figure 4.12 (b), as indicated by a significant drop in loading in figure 4.11. This debonding is critical and severely affects the structural integrity and load-carrying capacity of sandwich composite structures. This debonding of face sheet and core should be avoided with all eventuality to determine the safe life and reliability of high-risk laminated sandwich composite structures, which might otherwise lead to a catastrophic failure of the whole system.

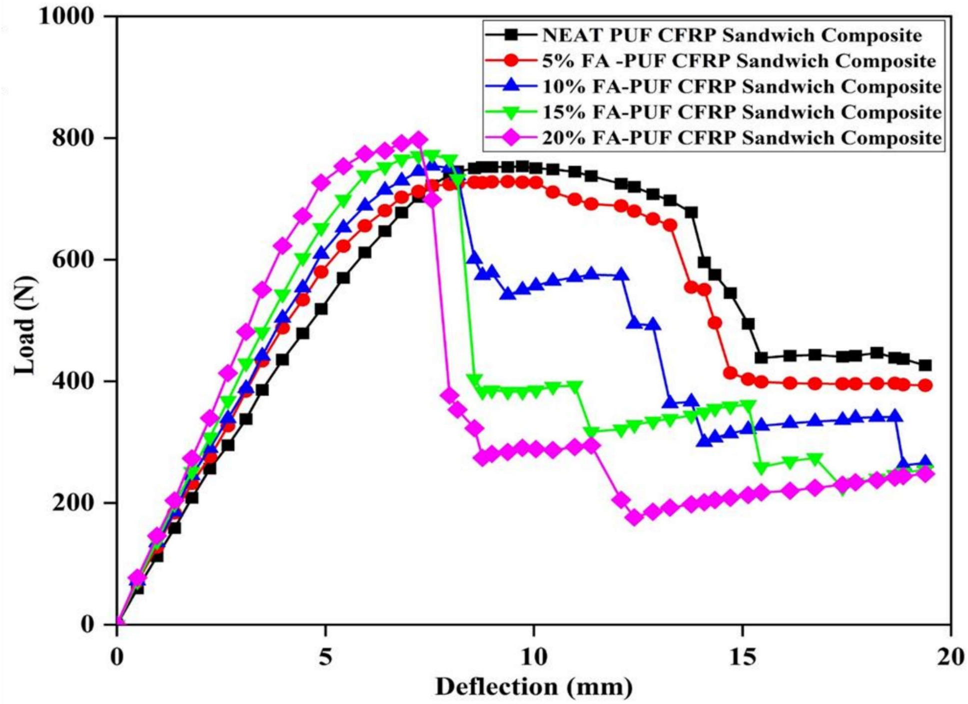

Figure 4.11 Load- Deflection curve of FA-PUF CFRP sandwich composite under bending.

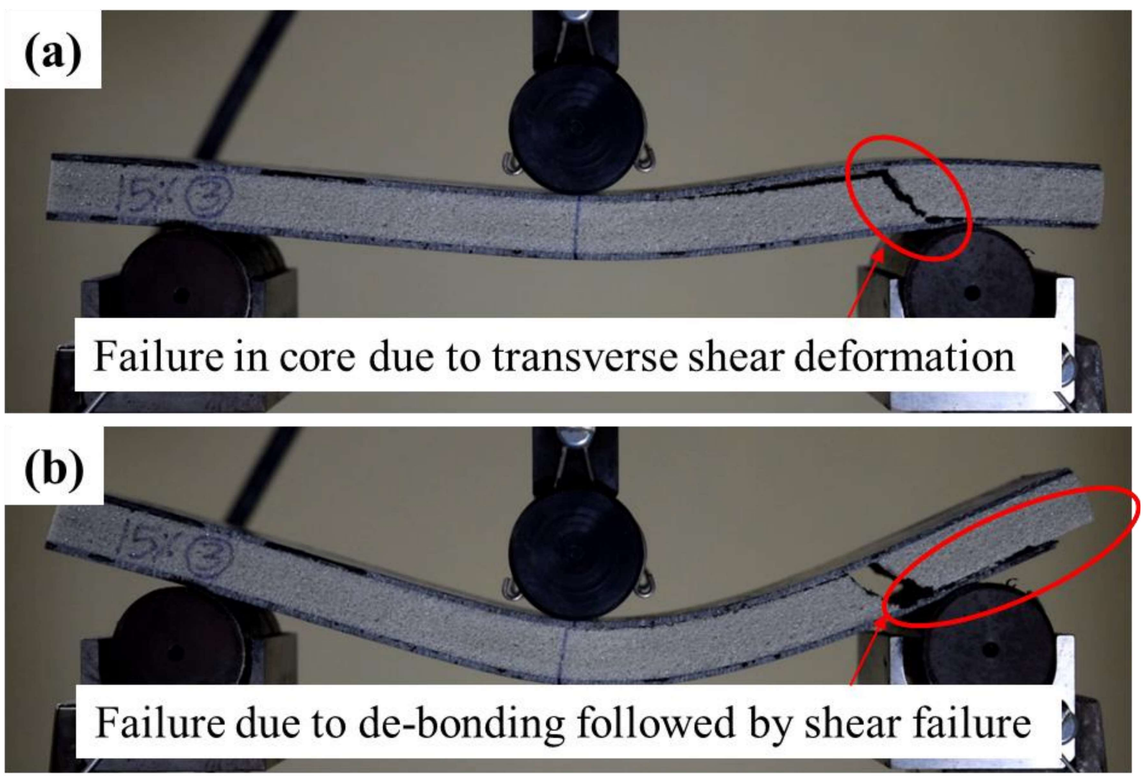

Figure 4.12 (a) Shear failure of sandwich composite under bending (b) Debonding of bend specimen.

Table 4.4 Variation of Peak values of bending load and corresponding deflection of GFRP and CFRP sandwich composites with weight % fly ash inclusion.

Varying fly ash weight percentage	**GFRP Sandwich Composite**		**CFRP Sandwich Composite**	
	Peak Bending Load (N)	**Deflection at Peak Load (mm)**	**Peak Bending Load (N)**	**Deflection at Peak Load (mm)**
NEAT PUF	630.40	7.57	753.12	9.72
5% FA-PUF	627.20	7.57	728.29	9.37
10% FA-PUF	633.65	7.94	754.12	7.55
15% FA-PUF	653.29	7.30	772.58	7.55
20% FA-PUF	699.30	5.62	797.36	7.22

4.3. Scanning Electron Microscope Analysis and Reinforced Mechanism of Fly Ash to PUF Core

The close cell PU foam structure is composed of cell struts and cell walls. The different volume fraction of the polymer constitutes the cell struts and the cell walls in the PUF architecture. Prime load-carrying member being strut, they sustain bending load while walls undergo stretching. When the polyurethane is reinforced with fly ash, the FA particles are distributed to the cell struts and cell walls. FA particulate is the discontinuous phase and PU is the continuous phase. Now, so synthesized FA-PUF is addressed as particulate reinforced polymer matrix composite. The elastic modulus and load-carrying capacity of FA-PUF increases with the percentage increase in the reinforcement with a limit controlled by the agglomeration and rigidity of the structure. The reinforcement particles must be small enough to act as reinforcement in foam composite. Evidently, only those particles small enough can enter the struts which form the skeleton of the foam composite [94]. FA particles enter the cell struts and strengthen the struts that strengthen the overall FA-PUF. This FA reinforcement is distributed among the struts and cell walls, inducing an increase in elastic modulus and strength. Since interface adhesion condition determines the stress transfer between the reinforcement and matrix, so surface treatment employing silane solution such as GPTS is used to improve the FA-PUF interface and its adhesion characteristics.

Figure 4.13 shows the scanning electron microscope images of variation of cell size with respect to fly ash wt.% inclusion to the PUF. Table 4.5 gives measured average cell sizes corresponding to different fly ash inclusion. All cells are observed to be polyhedral, whether it is neat PUF or PUF reinforced with FA. The size of the cells decreased with the increase in FA weight percent inclusion because the volume of the mould is constant for the expansion of the Polyol and MDI mixture. The amount of Polyol and MDI is the same for the fabrication of PUF neat and FA-PUF. The decrease in cell size implies an increase in cell numbers per unit volume of PUF. This increase in cell numbers leads to a decrement in cell wall and strut thickness. This decrement results in the degradation of the mechanical properties of FA-PUF core. Cell wall thickness criterion is more dominant than the fly ash reinforcement; due to this initially there is a drop in shear strength observed. But as the inclusion is uniformly distributed to the cell walls, subsequently, the gain in shear strength was reported. This strengthening has also been reflected in the earlier results of the shear stress-strain curve in figure 4.8 and table 4.3, where the FA-PUF strength was seen to be first decreased in comparison with neat PUF. Subsequently, beyond 15% inclusion, the enhancement of mechanical property is observed. Thereafter shear modulus is increased as the inclusion of FA in PUF increases. This can be concluded that although the cell density influences the mechanical property of FA-PUF structure, but the fundamental mechanism for property improvement being the synergic effect of FA and PUF in the structure[206]. The rise in weight percentage of FA in PUF leads to enhancement of the elastic property, if distributed uniformly in the cell structure and confers in the degradation of the property when agglomerated. The SEM images in figure 4.14 shows the fly ash distribution in PU foam cells.

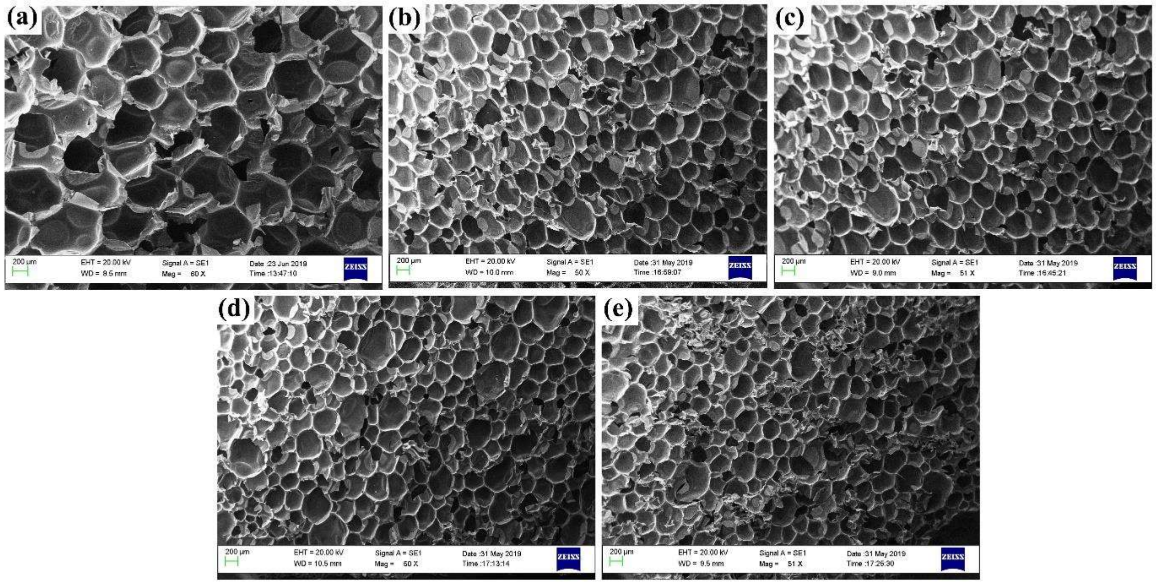

Figure 4.13 SEM images of (a) Neat PUF, (b) 5% FA-PUF, (c) 10% FA-PUF, (d) 15% FA-PUF and (e) 20% FA-PUF.

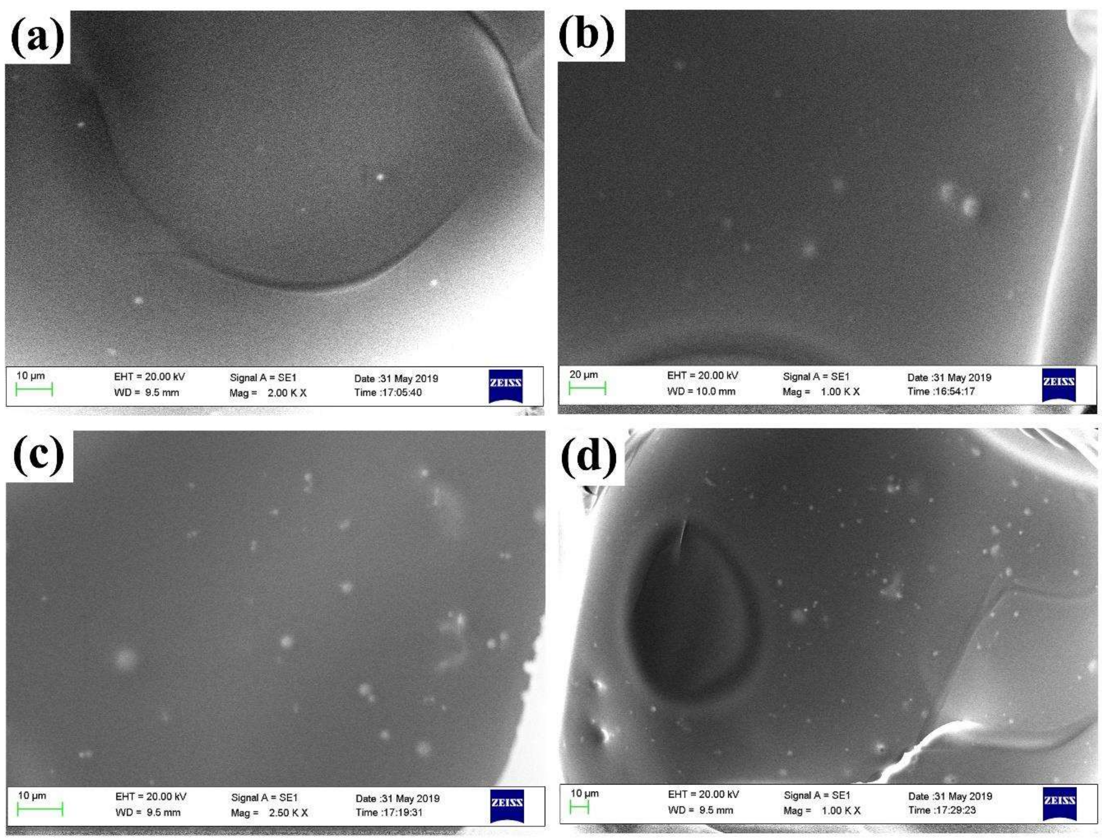

Figure 4.14 SEM images of fly ash distribution in polyurethane foam core cell (a) 5% FA-PUF, (b) 10% FA-PUF, (c) 15% FA-PUF and (d) 20% FA-PUF.

Table 4.5 Average cell size of different weight % FA-PUF.

Sample Name	Average Shell Size (mm)
Neat	615.86 μm
5% FA-PUF	426.25 μm
10% FA-PUF	410.21 μm
15% FA-PUF	363.12 μm
20% FA-PUF	337.11 μm

From the SEM images, it is realized that the fly ash is uniformly distributed through the cell geometry. All the foam core and FRP sandwich laminated composite specimens prepared and tested in this work possess this uniform distribution pattern of fly ash. The variation in strength with inclusion was well justified with the scanning electron microscopy. The favourable results provide a strategy to utilize the low-cost fly ash in sandwich composite structural applications, thereby even getting rid of the negative impact on the environment of this industrial by-product. Results obtained indicate that the change in polyurethane core property largely depends on the fly ash inclusion and cell size of the core. PUF cell size was reduced with the fly ash inclusion. Shear modulus of core surged with the addition of fly ash and the same trends were also observed for the bending stiffness of the beam.